Experiments on animals and animal tissues

It is a requirement of the Society that all vertebrates (and Octopus vulgaris) used in experiments are humanely treated and, where relevant, humanely killed.

To this end authors must tick the appropriate box to confirm that:

For work conducted in the UK, all procedures accorded with current UK legislation.

For work conducted elsewhere, all procedures accorded with current national legislation/guidelines or, in their absence, with current local guidelines.

Experiments on humans or human tissue

Authors must tick the appropriate box to confirm that:

All procedures accorded with the ethical standards of the relevant national, institutional or other body responsible for human research and experimentation, and with the principles of the World Medical Association's Declaration of Helsinki.

Guidelines on the Submission and Presentation of Abstracts

Please note, to constitute an acceptable abstract, the Society requires the following ethical criteria to be met. To be acceptable for publication, experiments on living vertebrates and Octopus vulgaris must conform with the ethical requirements of The Society regarding relevant authorisation, as indicated in Step 2 of submission.

Abstracts of Communications or Demonstrations must state the type of animal used (common name or genus, including man. Where applicable, abstracts must specify the anaesthetics used, and their doses and route of administration, for all experimental procedures (including preparative surgery, e.g. ovariectomy, decerebration, etc.).

For experiments involving neuromuscular blockade, the abstract must give the type and dose, plus the methods used to monitor the adequacy of anaesthesia during blockade (or refer to a paper with these details). For the preparation of isolated tissues, including primary cultures and brain slices, the method of killing (e.g. terminal anaesthesia) is required only if scientifically relevant. In experiments where genes are expressed in Xenopus oocytes, full details of the oocyte collection are not necessary. All procedures on human subjects or human tissue must accord with the ethical requirements of the Society regarding relevant authorisation, as indicated in Step 2 of submission; authors must tick the appropriate box to indicate compliance.

SA01

The biophysical basis of intracellular homeostasis

Peter Hunter[1]

[1]University of Auckland, New Zealand

Cellular physiology operates at the theoretical limits set by physical laws – for example, ion channels are sensitive to the passage of a single elementary charge, and retinae can detect one photon. Eukaryotic cells also exploit every form of energy storage mechanism available – biochemical (e.g., solute concentrations and chemical bonds), electrical (e.g., capacitive charge storage in the cell membrane), mechanical (e.g., the elastic compliance of cellular membranes), and thermal (the heat storage essential for maintaining body temperature). Since cells appear to have evolved to maximally exploit the laws of physics within their particular environmental niche, we should try to explain cell behaviour in the light of those laws.

This talk will present an analysis of cell homeostasis using a 'bond graph' modelling approach that ensures that the conservation laws of physics (i.e., conservation of mass, charge, and energy, respectively) are satisfied for the interdependent biochemical, electrical, mechanical, and thermal energy storage mechanisms operating within the cell. The bond graph approach is applied to several cell membrane transport mechanisms and then used to consider how physics constrains intracellular electrolyte homeostasis for enterocytes (the epithelial absorptive cells in the lining of the intestinal mucosa). The model includes the electrogenic sodium-potassium ATPase pump (NKA) and an inwardly rectifying potassium channel (Kir) in the basolateral membrane, the electrogenic sodium-driven glucose transporter (SGLT1) in the apical membrane, and the glucose transporter (GLUT2) expressed in both membranes.

Glycolysis converts the imported glucose to ATP to drive NKA. For specified levels of sodium (Na^+), potassium (K^+), and glucose in the blood, the model demonstrates how enterocytes absorb Na^+ and glucose from the lumen and transfer glucose to the blood while maintaining the membrane potential and homeostasis of intracellular Na^+ and K^+. The Gibbs free energy available from the ATP hydrolysis ensures that the cell operates as a 'sodium battery' with a high external to internal ratio of Na^+ concentration in order to provide the energy for many other cellular transport processes. We show balanced homeostasis of Na^+, K^+, glucose, ATP, and membrane potential under varying levels of glucose in the lumen. We demonstrate that this balance is due to the 3:2 stoichiometry of Na^+/K^+ exchange in NKA, the 2:1 Na^+/glucose cotransport in SGLT1, the 1:2:2 ratio between glucose consumption, ATP, and water production in glycolysis, the K^+ efflux through Kir, and the glucose transport via GLUT2. We analyse the energy costs of varying the ratio of GLUT2 to SGLT1 in the apical membrane of the enterocyte. We also show how the flux for SLC transporters, ATPase pumps and ion channels can be expressed in a consistent and thermodynamically valid expression.

A bond graph approach captures the laws of physics at the appropriate scale for understanding physiological mechanisms. In the example presented here, a biophysical analysis of enterocyte homeostasis provides a quantitative explanation for the variable and transient expression of GLUT2 transporters, against the background of SGLT1 expression, under varying post-prandial levels of glucose and sodium in the intestinal lumen.

SA02

Adaptation to stress: Why reduction ain't the answer

Michael Joyner[1]

[1]Mayo Clinic, USA

In this talk I will discuss some of the multimodal and multiscale adaptations that animals (especially humans) make to stressors like exercise and hypoxia. I will also highlight that many insights come from 1) observational studies in a small number of animals or subjects, and 2) unusual patients that serve as human "knockouts" to test ideas about causality. A third point I will make is that physiology in specific and biomedical research in general needs to more fully leverage the August Krogh Principle as opposed to continuing to rely on narrowly focused and frequently inbred model systems. The goal of the talk is to be intentionally provocative.

SA03

Lessons learned from pacemaking: more players for a single function, more functions for a single player

Dario DiFrancesco[1]

[1] University of Milan, Italy

Pacemaking, a most fundamental cardiac function, has long occupied a central place in physiological research. What makes the heart "beat"? Spontaneous activity originates in SAN pacemaker cells thanks to a distinctive phase of their action potentials, the diastolic depolarization (DD). In the late 70s, a new ionic current ("funny", If current), was identified in pacemaker tissue. Its unusual property (an inward current activated on hyperpolarization) introduced a novel concept in pacemaker physiology in strong contrast with existing models. Subsequent studies of If and its molecular correlates, the HCN channels, established their key role in DD generation and in autonomic modulation of heart rate. Pacemaking is however a complex cellular process, and other players are known to contribute, including the Ca-clock mechanism, the sustained inward current, the ACh-activated K current, the Cav1.3 channel; this latter player, expressed exclusively in pacemaker cells, has distinctive properties and according to recent data fully controls, together with HCN4 channels, adrenergic rate modulation. Although specific functional aspects may require fewer mechanisms, the whole pacemaking function emerges from the coordinated action of many players. This raises two questions: 1) why several players for a single function? 2) if one function needs several players, how extensive must the repertoire be to support the extraordinarily large number of cellular functions?

The answer to 1) is "robustness": redundancy ensures that backup mechanisms compensate when one or more components fail. The answer to 2) is "multifunctionality": many molecular players serve diverse roles across tissues. f/HCN channels, for example, are expressed far beyond cardiomyocytes and participate in processes as varied as sensory transduction, hormone secretion, gastrointestinal motility, osteoclastogenesis, immune cell activation, mitochondrial respiration, even stem-cell cycle control and early embryonic development, and others.

The lessons learned from these studies illustrate a general principle: biological functions arise from combinatorial partnerships among mechanisms, rather than from a simplistic "one gene–one function" paradigm.

SA04

Linking wet and dry lab to control rhythm disturbances

Jakub Tomek[1]

[1]University of Oxford, United Kingdom

Computational modelling has become an integral component of modern cardiovascular research, from academia to industry. Beyond their predictive capabilities, simulations now play a central role in shaping scientific investigation: generating hypotheses that can be tested experimentally and providing frameworks to interpret resulting data. Crucially, computer models are valuable not only when they agree with experimental data, but also when they disagree. Such discrepancies are often the most informative, revealing gaps in our current understanding of complex physiological systems.

To demonstrate the benefits of integrated dry-and-wet-lab approaches, I will focus on two areas. First, I will argue that improving data quality is currently more critical than improving computer models for better in silico drug safety and efficacy studies, and propose a strategy whereby computer models actively guide new data acquisition. Second, I will demonstrate how simulations and experiments can be used synergistically to maximise relevance of animal and in vitro models for human health, enhancing both mechanistic understanding and translational value.

I will conclude by outlining key future directions for integrated dry-wet lab studies, including the development of more general and life-like virtual cells, bridging subcellular to tissue phenomena, and the integration of physiology-based modelling with emerging AI-driven approaches.

SA05

"A Device for Dynamic FAD Measurements in the Human Heart Ex Vivo Model and an In Vivo Large Animal Model"

Eric Rytkin[1], Nathaniel Quirion[2], Luyao Lu[2], Igor Efimov[1]

[1]Northwestern University, United States, [2]George Washington University, United States

Introduction:

We have developed an implantable device for dynamic flavin adenine dinucleotide (FAD) measurements in cardiac tissue. FAD fluorescence provides a label-free optical readout and can be used to assess metabolic changes during ischemia, reperfusion, and pharmacologically induced alterations in coronary perfusion. The device is designed for direct placement on the heart surface, enabling real-time monitoring of relative FAD levels in both ex vivo and in vivo cardiac models.

Aims:

The aim of this study was to perform dynamic FAD measurements from the heart using an implantable, suturable device format. This approach was designed to enable continuous monitoring of changes in myocardial FAD levels under controlled ischemic and perfusion-modifying conditions.

Methods:

FAD measurements were performed in one canine model, two porcine models, and one declined donor human heart maintained in an ex vivo perfusion system. In the canine model, the obtuse marginal branch was ligated to mimic localized myocardial ischemia. In the porcine models, acetylcholine injections were performed to induce coronary vascular responses and assess corresponding changes in FAD signals. In the ex vivo human heart model, perfusion was transiently interrupted for defined intervals to evaluate changes in FAD levels during ischemia and reperfusion. The implantable LED sensor array was positioned on the epicardial surface to record dynamic relative FAD signals under these experimental conditions.

Results:

Dynamic changes in relative FAD levels were successfully recorded in both in vivo large animal models and the ex vivo human heart model. In the canine ischemia model, local coronary ligation produced measurable alterations in FAD signal consistent with regional metabolic changes. In the porcine models, acetylcholine administration was associated with detectable changes in relative FAD levels during pharmacologically induced vascular responses. In the ex vivo human heart, transient interruption and restoration of perfusion resulted in dynamic FAD signal changes during ischemia-reperfusion intervals.

Conclusions:

This study demonstrates the feasibility of an implantable, suturable cardiac sensor array for dynamic measurement of relative FAD levels on the heart surface. The device enables real-time assessment of metabolic changes in both in vivo large animal models and an ex vivo human heart preparation. These findings support further development of implantable optical technologies for monitoring myocardial metabolism during ischemia, reperfusion, and altered coronary perfusion.

The animal studies were performed in compliance with animal protocols. The human donor heart was declined for transplant and hereby considered discarded tissue.

https://www.science.org/doi/full/10.1126/sciadv.ads8608 - features the previous version of the device.

C01

Artificial Intelligence-Enabled Reconstruction of Beat-by-Beat Cardiomyocyte Nano-Dynamics Reveals Mechanical Auto-Regulation of Cardiac Function

Eva Rog-Zielinska[1]

[1]Institute for Experimental Cardiovascular Medicine, University of Freiburg, Germany

The external appearance of uniformity of cardiomyocyte contractions emerges from coordination of numerous, spatio-temporally heterogeneous processes, involving specialised sub-cellular nano-domains. Through omnidirectional coupling of electrical activity, calcium fluxes, and mechanical action, cardiomyocytes rapidly adjust to ever-changing physiological demand. It remains unknown how dynamic ultrastructural cross-talk contributes to the marked cardiac auto-regulatory capacity.

I propose that beat-by-beat auto-regulation of heart function is governed at the nano-scale by a process unique to cardiomyocytes: the rhythmic cycle of cardiomyocyte stretch, contraction, and relaxation. In this concept, the heartbeat is not merely the consequence of cardiomyocyte activity, but an intrinsic regulator that continually modifies nano-domain structure and function in preparation for the next beat.

In order to understand beat-by-beat cardiomyocyte nano-dynamics, we combine time-resolved 3D electron tomography, sub-cellular functional imaging, and artificial intelligence-assisted segmentation of cardiomyocyte sub-cellular ultrastructure, where deep learning-based segmentation enables automated reconstruction of complex cardiomyocyte ultrastructural components. Finally, we use artificial intelligence-based generative models and computational modelling for data synthesis, and for testing and generation of new hypotheses.

We have shown that cardiomyocyte contraction and stretch are associated with beat-by-beat deformation of cardiomyocyte organelles: transverse-axial tubular system (TATS), sarcoplasmic reticulum, mitochondria, microtubules, caveolae, and nuclei. In order to visualise cardiomyocyte contraction on the nano-scale (something that would be impossible experimentally) we used generative adversarial models to synthesise biophysically constrained ‘motion pictures’ of cardiomyocyte ultrastructure with nanometre-resolution, creating a powerful hypothesis-generation platform linking nanoscale structural deformation to electro-mechanical function.

As an example of a functional relevance of organelle deformation, we have shown that TATS (a network of surface membrane invaginations that enables close structural coupling of plasma membrane and extracellular fluid with sarcoplasmic reticulum) cyclically deforms during cardiomyocyte stretch and contraction in rabbit (all investigations conformed to national and international animal welfare laws). Cyclic, beat-by-beat TATS deformation which is associated with faster luminal content exchange with the bulk extracellular space, an effect that scales up with contraction amplitude and frequency. TATS ‘pumping’ serves to abolish intraluminal calcium depletions that would otherwise develop as a consequence of transmembrane calcium fluxes, and – if left unrectified by deformation-driven pumping – would lead to the loss of the contractile force.

In conclusion, our studies represent an innovative framework that can provide unique insights into the nanoscopic dynamics of cardiomyocytes. Cardiac organelle mechano-sensitivity likely represents a fundamental principle of cardiac physiology, where mechanical modulation of nano-domain structure and function can help us understand how cardiomyocytes adapt rapidly to changes in circulatory demand.

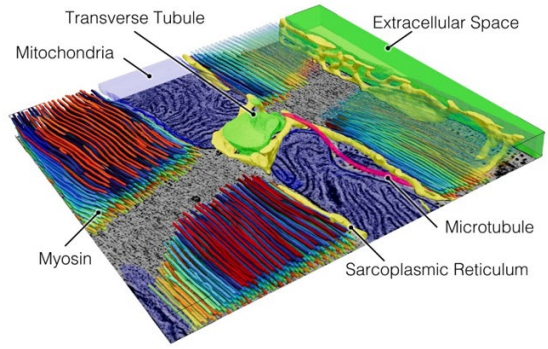

3D model of the sarcoplasmic reticulum (yellow) and transverse tubules (green), microtubules (magenta), mitochondria (transparent blue), and myosin (depth-position color-coded), constructed using artificial intelligence tools.

C02

Glycocalyx Integrity Associates with Diastolic Function and is Therapeutically Targetable in Cardiometabolic Diseases

Stanley Buffonge[1], Yan Qiu[1], Emma Hart[1], Rebecca Foster [1], Simon Satchell [1]

[1]University of Bristol, United Kingdom

Introduction:

Damage to the coronary microvascular endothelial cell (CMVEC) glycocalyx has been implicated in cardiometabolic disease and may contribute to microvascular dysfunction. The glycocalyx is a complex and dynamic structure composed of proteoglycans and glycoproteins and plays a key role in regulating vascular permeability. Given the sensitivity of the myocardium to alterations in microvascular barrier function, disruption of the glycocalyx may be linked to impaired cardiac relaxation. However, its relationship with diastolic dysfunction across cardiometabolic conditions and its responsiveness to therapeutic intervention remain incompletely understood.

We aimed to determine whether glycocalyx integrity is associated with diastolic function in experimental models of cardiometabolic disease and to assess whether pharmacological interventions that preserve the glycocalyx are accompanied by improvements in cardiac function.

Methods:

In vitro: Human CMVEC were treated with 10ng/ml of TNF-α for 6 hours and treated with the MMP2/9-specific inhibitor, SB-3CT (10mg/ml) or finerenone (3mM). Quantitative PCR arrays, immunofluorescence, and ELISAs were used for investigation.

In vivo: Type 1 diabetes was induced in male FVB mice by injection of streptozotocin (STZ). Diabetic mice were treated with SB-3CT (10mg/kg), daily for 2 weeks from 7 weeks post STZ. In a second model, aged female mice (~17–20 months), were fed on a high fat diet or control low fat diet for 12 weeks. After 8 weeks, mice were given finerenone at 2 mg/kg/day orally for 4 weeks. Echocardiography was utilised to assess diastolic function. Lectin staining was conducted on heart tissue to give an indication of glycocalyx depth.

Results:

TNF-α significantly increased MMP-9 and heparanase mRNA expression ($p<0.01–0.001$) and promoted shedding of syndecan-4 (SDC4) and glycosaminoglycans into the conditioned media ($p<0.05–0.001$), alongside reduced cell surface SDC4 expression ($p<0.05$). Treatment with the MMP-2/9 inhibitor SB-3CT attenuated SDC4 shedding and restored surface expression ($p<0.01$), while both SB-3CT and finerenone reduced glycosaminoglycan shedding ($p<0.05–0.01$). Finerenone also significantly suppressed TNF-α-induced heparanase expression ($p<0.001$), supporting a protective effect on glycocalyx integrity under inflammatory conditions.

In vivo, streptozotocin-induced diabetic mice exhibited diastolic dysfunction, evidenced by a reduced E/A ratio (n=10 for controls and 5 for diabetes; control: 2.0±0.12 vs diabetes: 1.5±0.09; $p<0.05$), accompanied by reduced glycocalyx depth (n=5, control: 279.4±11.7 nm vs diabetes: 158.7±30.2 nm; $p<0.05$), increased cardiac MMP-9 activity, and enhanced vascular permeability as indicated by albumin extravasation. Treatment with SB-3CT restored glycocalyx depth (n=5 for SB-3CT + diabetes; 270.3±31.3 nm; $p<0.05$), improved diastolic function (E/A: 2.2±0.15; $p<0.05$), reduced MMP-9 activity ($p<0.01$), and decreased albumin leakage. Glycocalyx depth was positively correlated with diastolic function, while cardiac MMP-9 activity was negatively correlated ($p<0.05$).

In a complementary model, aged female mice subjected to high-fat diet feeding developed diastolic dysfunction, which was significantly improved following finerenone treatment (n=6 for all groups, $p<0.05$) without alterations in blood pressure.

Conclusion:

Glycocalyx integrity is closely associated with diastolic function across distinct cardiometabolic models and is responsive to pharmacological intervention. These findings support the glycocalyx as a central marker of coronary microvascular health and a potential therapeutic target in diastolic dysfunction.

C03

Investigating the role of nerve growth factor in neuro-cardio-vascular co-development in a human 3D innervated cardiac muscle model

Michael Gani Setya[1], Lennart Valentin Schneider[1], Aditi Methi[2], André Fischer[2], Daniel Härtter[1], Maria-Patapia Zafeiriou[1]

[1]Institute of Pharmacology & Toxicology, Germany, [2]German Center for Neurodegenerative Diseases (DZNE), Germany

Nerve growth factor (NGF) is a neurotrophin essential for the differentiation and survival of sympathetic neurons (SNs). In the developing heart, NGF released by perivascular cells orchestrates sympathetic innervation. To model this process *in vitro*, we established a 3D innervated engineered heart muscle (iEHM) by fusing human iPSC-derived sympathetic neuronal organoid (SNO) with engineered heart muscle (EHM). Optogenetic SYN-f-Chrimson SNO fused to the EHM increased beating rate upon light stimulation, demonstrating functional connectivity between SNs and cardiomyocytes (n=41 iEHMs, 3 independent differentiations).

To investigate the cellular composition of this system, single-nuclei RNA sequencing (snRNA-seq) was performed, revealing co-development of vascular and perivascular cells. These findings were validated by immunofluorescence that showed a dense vascular network ($PECAM1^+$), supported by pericytes ($PDGFR\beta^+$) interlaced with neurons and sympathetic varicosities ($TH^+/SYN1^+$), suggesting close neuro-vascular interactions. Quantitative analysis using machine learning–based orientation and proximity analysis demonstrated a strong directional correlation between SNs and vessels. Furthermore, snRNA-seq identified perivascular cells as the main source of NGF, consistent with *in vivo* data.

To dissect the specific role of NGF in neuro-cardio-vascular development, we engineered a doxycycline-inducible NGF (iNGF) hiPSC line using CRISPR/Cas9. The TET-ON iNGF system, integrated at the AAVS1 locus, couples a NGF coding sequence with a GFP reporter. iNGF-EHMs were fused with optogenetic SNOs and cultured for 4 weeks under NGF induction of 0, 1, 2, or 3 weeks (n=10-11 iEHMs per condition). Light stimulation over 3 weeks NGF induction significantly increased the beating rate, while contractile performance significantly decreased in 2- and 3-week iNGF tissues. Immunofluorescence further showed hyperinnervation (TH^+/NF^+) of cardiomyocytes ($CTNT^+$) after 1–2 weeks of NGF induction, which declined in 3-week iNGF tissue. Orientation/proximity analysis across doxycycline-treated versus control tissues (n=7-13 imaging fields) revealed reduced neuro–vascular alignment after prolonged NGF induction, supporting the concept that pericyte-derived NGF attracts neuronal axons.
Together, the iNGF-iEHM represents a robust *in vitro* human model to dissect NGF-dependent mechanisms of sympathetic innervation and neuro-cardio-vascular development. Our results demonstrate acute NGF induction enhances neuro-cardiac connectivity, while chronic exposure disrupts its contractile performance. These findings highlight that balanced neurotrophic signaling is essential for coordinated cardiac development and establish a platform to investigate NGF-driven mechanisms underlying cardiac dysfunction.

C04

Redefining neurocardiac interactions in the human heart

David Revuelta[1], Corey Smith[2], Johanna Bufler[1], Rebecca Jark[1], Brunetti Andrea[1], Anna Zerio[1], Eric Jacquet[3], Evaldas Girdauskas[4], Cristina Molina[1]

[1]Institute of Experimental Cardiovascular Research - University Medical Center Hamburg-Eppendorf (UKE), Hamburg, Germany, [2]Department of Physiology, Case Wester Reserve University, Cleveland, OH, United States, [3]Université Paris-Saclay, CNRS, Institut de Chimie des Substances Naturelles, Gif-sur-Yvette, France, [4]University Heart & Vascular Center Hamburg - University Medical Center Hamburg-Eppendorf (UKE), Hamburg, Germany

The heart is innervated by a sympathetic neuronal network that regulates its function, especially during conditions of increased physiological demand such as stress or exercise. Increased sympathetic activation is a hallmark of several cardiovascular diseases and arrhythmias. However, little is known about the physiological mechanisms underlying sympathetic control of the heart, hyperactivation or hyperinnervation. Although significant progress has been made in understanding heart function, including the neurohormonal effects in the cardiomyocytes, understanding direct neuro-cardiac coupling mechanisms and the influence of neuronal density, contact and remodelling has been challenging. The aim of this study was to investigate neuro-cardiac interactions for the first time human primary cardiac neurons and myocytes .

Human atrial discarded tissue was obtained during cardiac surgery from 42 patients. Tissue samples were cleared of adipose tissue and only myocardium sections were used for cells isolation. Cells were then transduced with adenoviral vectors, encoding for the fluorescence resonance energy transfer (FRET) biosensor Epac1-camps, for real-time live-cell measurement of cytosolic cyclic adenosine monophosphate (cAMP)[1], and cultured during 48h as previously described[2]. Traditionally, neuronal somas are thought to be restricted to the central nervous system and the ganglia. However, we found a large population of functional resident neurons spread through the myocardium. We then co-cultured intracardiac neurons and myocytes and compared the FRET response to increasing concentrations of isoprenaline (1, 10 and 100 nM), a β-adrenergic agonist. Additionally, the cAMP-degrading capacity was assessed by measuring the response to 100 µM 3-isobutyl-1-methylxanthine (IBMX), a non-specific phosphodiesterase inhibitor, under isoprenaline stimulation and basal conditions. cAMP increase in response to 1 nM isoprenaline was not significantly different in isolated myocytes compared to those in contact with neurons (2.52 ± 0.63% *vs*. 6.40 ± 1.30%, p=0.126) but it was significantly greater at 10 nM (7.97 ± 1.63% *vs*. 14.36 ± 2.43%, p = 0.036) and 100 nM (14.08 ± 2.20% *vs*. 25.40 ± 4.20%, p=0.004). Importantly, cAMP increase to 1 nM isoprenaline in myocytes that were in contact to neurons was similar to the maximal response of 100 nM isoprenaline in myocytes alone. IBMX response was also stronger in myocytes in contact with neurons both in isoprenaline stimulation (21.58 ± 3.45% *vs*. 30.05 ± 5.09%, p=0.028) and basal conditions (15.39 ± 4.98% *vs*. 51.17 ± 5.97%, p<0.001), an effect that can only be explained by sympathetic neurotransmission. Normal distribution was confirmed by Shapiro-Wilk test. Data are expressed as mean ± standard error of the mean. Linear mixed models were used employing estimated marginal means as post-hoc test to obtain the p-values of pairwise comparisons.

These findings suggest that efficient sympathetic regulation of cardiac function occurs *via* direct coupling between myocytes and intracardiac neurons. The existence of this neuronal network and extensive cell-cell interactions could resolve the precise, specific and temporally tuning of heart function and provide the mechanistic framework for some cardiac arrhythmias.

C05

Association between sympathetic nervous system dysregulation and ventricular arrhythmogenesis in a progressive murine model of chronic kidney disease

Katie Tompkins[1], Abbie Hayes[1], Joanne L Mitchell[1], Olivia Baines[1], Rina Sha[1], Sophie Broadway-Stringer[1], Michael Sagmeister[1], Rowan Hardy[1], Charles Ferro[1], John Townend[1], Claudio Mauro[1], G.Andre Ng[2], Katja Gehmlich[1], Davor Pavlovic[1], Christopher O'Shea[3]

[1]University of Birmingham, United Kingdom, [2]University of Leicester, United Kingdom, [3]University of Warwick, United Kingdom

Introduction

Chronic kidney disease (CKD) drives adverse cardiac remodeling, characterized by interstitial fibrosis, diastolic dysfunction, and increased arrhythmic susceptibility, even in early disease stages. Early-stage CKD is associated with a six-fold elevation in sudden cardiac death risk, predominantly due to ventricular arrhythmia. A hallmark of CKD is persistent sympathetic nervous system (SNS) over activation, which perturbs cardiac electrophysiological and mechanical properties. However, the mechanistic link between renal dysfunction, SNS dysregulation, and ventricular arrhythmogenesis remains incompletely understood.

Aim

To investigate CKD-induced SNS dysregulation and its contribution to ventricular arrhythmia susceptibility in murine hearts.

Materials and Methods

Female C57BL/6J mice were fed either 0.15% adenine (n = 11) or control chow (n = 13) for 7 weeks to induce CKD. Renal dysfunction was quantified using serum BUN, creatinine, and normalised kidney weight. Cardiac electrophysiology was assessed via in vivo ECG and ex vivo optical mapping, with ventricular arrhythmia susceptibility evaluated using programmed stimulation. SNS activity was determined by heart rate variability (HRV) and circulating noradrenaline levels (ELISA). Cardiac structure and blood pressure were assessed by echocardiography and haemodynamic measurements. Results are presented as control versus adenine.

Results

Adenine-fed mice demonstrated increased serum BUN (8.5±0.9mmol/L vs 23.4±6.0mmol/L, $p<0.0001$), elevated creatinine (14.6±3.7umol/L vs 39.4±23.9umol/L, $p<0.0001$), and reduced kidney weight (251.8±26.90mg/g vs 188.6±33.9mg/g, $p<0.0001$), confirming renal impairment.

Adenine diet reduced HRV (figure 1) (2.1±1.0ms vs 1.2±0.6ms, $p = 0.0007$) and markedly elevated circulating noradrenaline (figure 2) (326.7±12.6pg/ml vs 1275±25pg/ml, $p < 0.0001$), despite reduced heart rate (736.6±22.56bpm vs 703.4±33.0bpm, $p=0.0002$), suggesting impaired chronotropic responsiveness and autonomic dysfunction.

Electrophysiological alterations included P-duration shortening (12.3±0.7 vs 11.2±0.9ms, $p=0.0007$) and PR-interval prolongation (33.0±2.0ms vs 35.3±2.5ms, $p=0.0014$). Ex vivo optical mapping showed action

potential duration prolongation. For example, at 120ms pacing cycle length, there was a significant action potential duration prolongation at 30% (14.4±1.6 vs 18.7±3.9, p=0.002), 50% (27.6±4.9 vs 35.6±8.2, p=0.006) and 80% repolarisation (49.6±6.7 vs 58.4±12.4, p=0.04).

Furthermore, adenine mice displayed amplitude alternans, indicating beat-to-beat electrical instability, across pacing cycle lengths (p <0.0001). 58% of adenine hearts displayed pacing-induced arrythmias, primarily ventricular tachycardia (75%) and ventricular fibrillation (25%), compared to 0% of control. These changes occurred without overt structural remodelling or hypertension.

Conclusion

Adenine-induced CKD in mice leads to significant SNS dysregulation, alongside bradycardia, PR prolongation, prolonged action potential duration, electrical instability, and increased ventricular arrhythmias. The coexistence of sympathetic activation with bradycardia suggests impaired autonomic control and neuro-cardiac remodelling contributing to arrhythmogenesis.

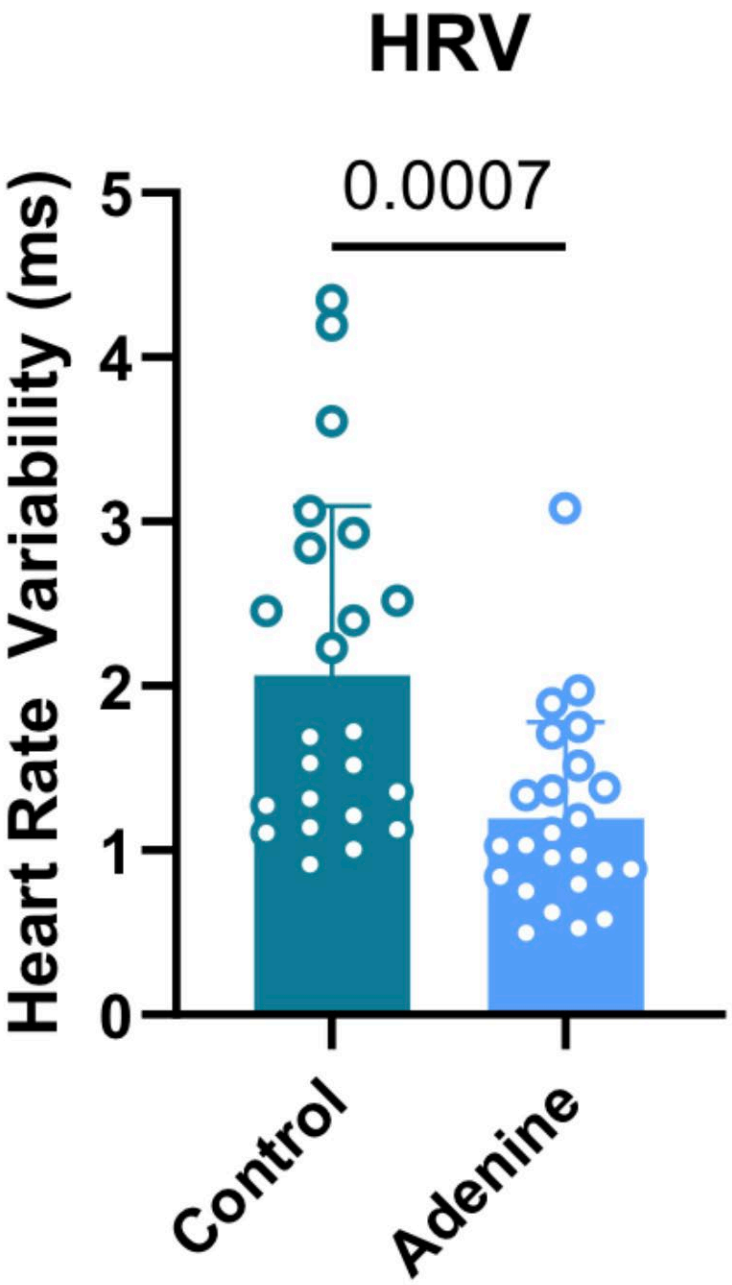
HRV
0.0007
Heart Rate Variability (ms)
0
1
2
3
4
5
Control
Adenine

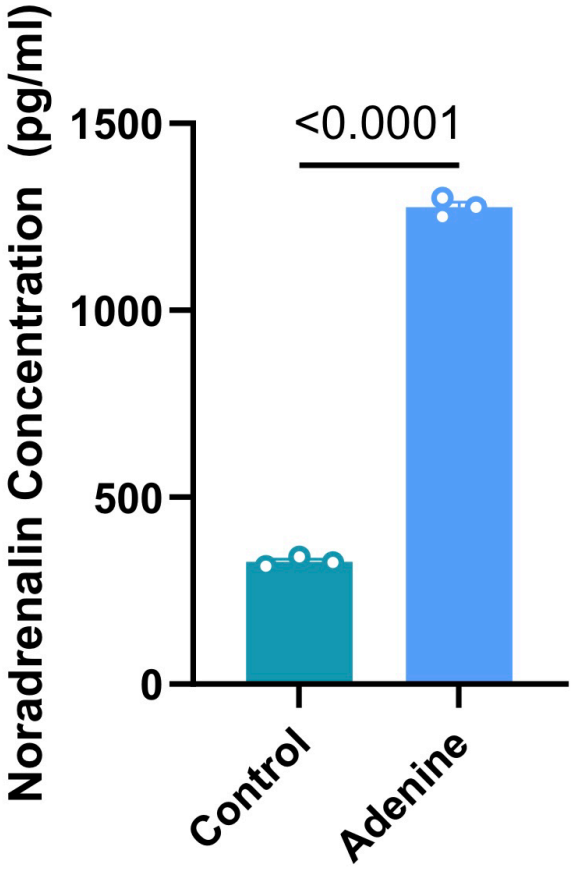
Noradrenalin Concentration (pg/ml)
1500
1000
500
0
<0.0001
Control
Adenine

C06

The effect of unilateral carotid body resection on beat-to-beat blood pressure variability in resistant hypertension

Marianna Theodorou[1], Lydia Simpson[1], Hazel Blythe[1], Laura Ratcliffe[2], Krzysztof Narkiewicz[3], Dagmara Hering[3], Zoar Engleman[4], Julian FR Paton[1], Emma C Hart[1]

[1]University of Bristol, United Kingdom, [2]University of Bristol and University Hospitals Bristol NHS Foundation Trust, United Kingdom, [3]Medical University of Gdansk , Poland, [4]Cibiem, United States of America

Background

The carotid chemoreceptors play an important role in cardiovascular regulation. In animal models of heart failure, heightened carotid chemoreflex activity is associated with increased blood pressure variability (BPV), which normalises following carotid body (CB) denervation (Del Rio, R. et al., 2013). In humans, higher beat-to-beat BPV indicates poor prognosis for cardiovascular mortality as it predicts increased risk for recurrent stroke and major cardiac events such as cardiovascular death and myocardial infarction (Webb, A.J.S. et al. 2018). Unilateral removal of CBs was shown to significantly reduce systolic blood pressure (SBP) in essential hypertensives, which was sustained in the long-term (mean ±SEM 3.1±0.6 years) follow-up investigation (Fudim, M. et al. 2015). However, whether beat-to-beat BPV is influenced by the carotid chemoreflex in humans is unclear. Therefore, the aim of this study was to retrospectively examine whether unilateral CB excision reduced BPV in people with drug resistant hypertension.

Methods

The data are from that published by Narkiewicz, K. et al. (2016), which complied with the Declaration of Helsinki and was approved by the Central Bristol research ethics committee. Fifteen people (7 males and 8 females) age 52 ±1 years with drug resistant hypertension participated in the study. Participants underwent unilateral carotid chemoreceptor excision. Beat-to-beat blood pressure was recorded during a 10-minute resting period (semi-supine) at baseline (pre-operative) and 3, 6 and 12 months post-operation. Beat-to-beat BPV was measured using average real variability (ARV) and the coefficient of variation (CoV) for both SBP and diastolic blood pressure (DBP). Only SBP ARV was normally distributed, ascertained by the Shapiro-Wilks test (alpha = 0.05), therefore all other data underwent logarithmic transformation. Data were then compared using a repeated measures one-way ANOVA with Dunnet's correction post-hoc comparisons. Data are presented as mean ± standard deviation (SD), unless otherwise stated.

Results

Resting SBP and DBP at baseline (pre-operative) were 165 ±38 mmHg and 81±24 mmHg. There was an effect of CB excision on the ARV for DBP (Figure 1, $p = 0.411$). The ARV of DBP was reduced from median 1.67 mmHg (interquartile range (IQR) 0.64) at baseline to median 1.26 mmHg (IQR 0.86) at 6 months post CB excision only ($p = 0.0411$). There were no differences in other measures of BPV from baseline to 3, 6 and 12 months post excision ($p > 0.05$).

Figure 1: **Average real variability of DBP at baseline vs post CB excision.** The ARV of DBP at baseline 0 months (2±1mmHg) is compared to 3 months (2±1mmHg); 6 months (2±1mmHg); and 12 months (2±1mmHg) post CB excision. Following logarithmic transformation, a repeated measures one-way ANOVA and post-hoc Dunnet's correction, only baseline vs 6 months post-CB excision was significant ($p = 0.041$) whereas baseline vs 3 months ($p > 0.05$) and baseline vs 12 months ($p > 0.05$) were not significant.

Conclusions

There was a reduction of DBP variability in resistant hypertensives at 6 months post-CB excision, suggesting that the CBs may contribute to BPV in humans. However, this needs further evaluation in a larger cohort to determine whether targeting the carotid body will improve BPV and prognosis in resistant hypertension.

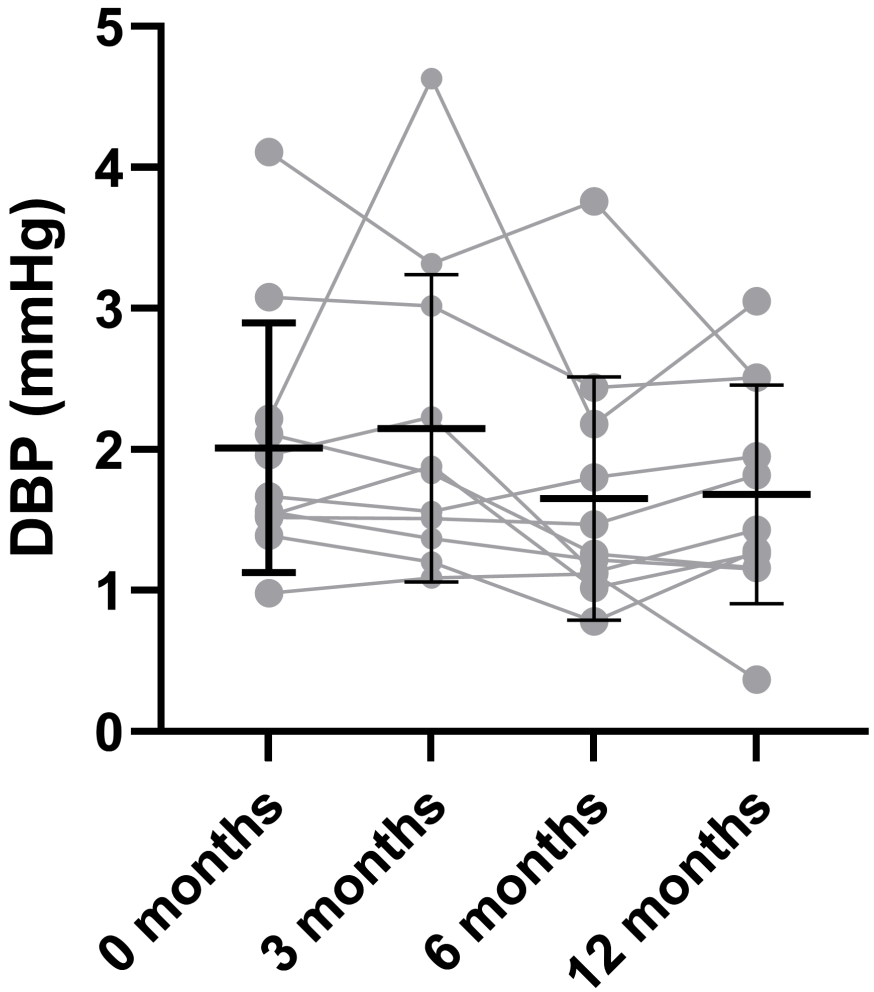

C07

The role of the carotid chemoreflex in the resting hyperventilation experienced by patients with long-COVID

Hazel C Blythe[1], Lydia L Simpson[1], Florence Mouy[1], Tim Swinn[1], Andy Shrimpton[1], Maria Pufulete[1], James W Dodd[1], Tim Robinson[2], James Thomas[1], Heidi Oliver[2], Adrian Kendrick[3], Julian FR Paton[4], Angus K Nightingale[5], Emma C Hart[1]

[1]University of Bristol, United Kingdom, [2]Sirona Care and Health, United Kingdom, [3]University of the West of England, United Kingdom, [4]University of Auckland, New Zealand, [5]University Hospitals Bristol and Weston NHS Foundation Trust, United Kingdom

Introduction

Long-COVID is a debilitating condition in which people continue to have health problems for months or years following COVID-19 infection. Long-COVID affects nearly 2 million people in the UK and costs ~£5.7 billion per year in productivity loss[1]. Many people with long-COVID experience ongoing breathing difficulties, despite having normal lung function and no evidence of gas exchange abnormalities. Evidence indicates that patients with long-COVID, who were not hospitalised for their initial infection, experience hyperventilation at rest and during exercise. The carotid chemoreflex plays an important role in the control of breathing at rest and during exercise[2] and its sensitivity was recently shown to be increased in people with long-COVID[3]. However, whether this hypersensitive carotid chemoreflex drives some of the hyperventilation experienced by patients with long-COVID remains unknown. Dopamine is used to inhibit carotid body afferent discharge into the brainstem, which inhibits the carotid chemoreflex response to hypoxia. However, some evidence suggests that dopamine signalling may be impacted in patients with long-COVID[4]. Thus, whether dopamine inhibits the carotid chemoreflex in patients with long-COVID is also unclear.

Objective

Dopamine will reduce carotid chemoreflex sensitivity in response to hypoxia and improve hyperventilation at rest in people with long-COVID, versus saline.

To determine whether inhibiting the carotid chemoreflex with low-dose dopamine can reduce heightened carotid chemoreflex sensitivity during hypoxia in people with long-COVID and improve their hyperventilation at rest.

Hypothesis

Methods

Six (2M, 4F, age; 50±9 years, BMI; 29.6±3.2 kg/m^2) participants with long-COVID completed resting ventilation measurements (during normoxia) and hypoxic ventilatory response (HVR) testing (measure of carotid chemoreflex sensitivity) during intravenous infusion of low-dose dopamine (2 mcg/kg/min) or saline (control) at rest. HVR was evaluated as the slope of the linear regression relating the minute ventilation to the nadir of oxygen saturation for each nitrogen exposure. Data were compared using Wilcoxon matched-pairs rank test. Data are reported as median (IQR).

Results

Intravenous dopamine reduced carotid chemoreflex sensitivity to hypoxia in people with long-COVID compared to saline (-0.15 (-0.17 to -0.09) L/min/SpO2% versus -0.36 (-0.79 to -0.20) L/min/SpO2%, P=0.0312, Cohen's D=1.061). Resting partial pressure of the end-tidal CO2 (PETCO2) tended to be increased with dopamine compared to saline (43 (41-44) mmHg versus 40 (38-42) mmHg), P=0.0312, Cohen's D=1.5), indicating a reduction in excessive hyperventilation at rest with dopamine.

Conclusion

Inhibiting the carotid chemoreflex with low-dose dopamine normalised HVR and improved hyperventilation at rest in people with long-COVID, versus saline. Tempering the carotid chemoreflex may be a viable treatment for people with long-COVID and unexplained dysregulation of ventilation.

C08

Occurrence and prevention of a novel class of ischaemia-reperfusion arrhythmias

Enaam Chleilat[1], Tony Rubio[1], Teo Puig Walz, Thomas Kok[1], Peter Kohl[1], Callum Zgierski-Johnston[1]

[1]Institute for Experimental Cardiovascular Medicine, University Heart Center Freiburg · Bad Krozingen Medical Center – University of Freiburg, Faculty of Medicine, Freiburg, Germany, Germany

Myocardial infarction is one of the leading causes of death and incapacity worldwide. Reopening the culprit artery to restore oxygenation is essential to prevent irreversible myocardial damage, but can also lead to deleterious events including arrhythmias. In previous work with rabbits, we identified a new type of ischaemia-reperfusion arrhythmia occurring in the myocardium along the main branch of the reperfused vessel ("perivascular excitation tunnelling", PVET) and showed that a 2-stage reperfusion method could prevent subsequent re-entrant arrhythmias.

Computational modelling of reperfusion using openCARP was performed. A simplified ventricular model was generated with an ischaemic area and a central channel representing the recovered myocardium around the reperfused vessel. With this model we could replicate PVET-induced arrhythmias and predicted that the size of the ischaemic area is a major determinant of arrhythmia likelihood. Prior work comparing small versus large rabbit hearts showed that larger hearts were indeed more likely to have re-entrant arrhythmias.[1]

To assess possible clinical relevance, as well as to identify whether risk scales with heart size across species, we performed experiments in pig hearts. All investigations conformed to German animal welfare laws and were performed with ethical approval by the local Institutional Animal Care and Use Committee (Regierungspräsidium Freiburg, X-21/03B). Explanted pig hearts were Langendorff perfused with HEPES-buffered physiological solution and optical mapping of transmembrane voltage performed. A cannula was inserted into a coronary artery and local ischaemia was achieved by perfusion of a simulated ischaemic solution (high K^+/low O2 solution). Reperfusion was performed either by reperfusing the whole ischaemic area at once (1-stage), or in a sequential manner (2-stage, with the cannula initially pushed deep into the artery for the first reperfusion step, and subsequently returned to the original position).

We confirmed the presence of PVET in pig hearts, characterised by the preferential recovery of myocardial excitability along the main branch of the reperfused vessel. In hearts reperfused with the 1-stage method, PVET occurred in 11 of the 12 hearts, resulting in re-entrant arrhythmias in 7 cases (N=12). The likelihood of PVET-driven re-entrant arrhythmias in the pig heart was no higher than in the rabbit heart, indicating that ischaemic size alone is not a sufficient parameter to predict arrhythmia. With the 2-stage protocol, PVET occurred in 4 of 6 hearts, but no re-entrant arrhythmias were observed. Thus, the two-stage protocol did not significantly alter PVET likelihood but did reduce the likelihood of re-entrant arrhythmias (p-value: 0.038; Fisher's exact test). We are currently optimising the computational model to incorporate realistic vasculature geometries and species differences. Finally, we are testing a new catheter, developed together with OSYPKA AG, to assess the efficacy of a 2-zone reperfusion method in a preclinical setting, which involves two separately controlled flow beds, enabling simultaneous

reperfusion with different solutions preventing a delay in tissue re-oxygenation. In the future, we hope to use imaging approaches and computational modelling for risk stratification to identify which patients would benefit from use of this catheter during percutaneous coronary intervention following myocardial infarction and thereby improve patient outcomes.

C09

Detection of exercising ectopic atrial and ventricular beats using non-linear analysis of clinically normal racehorse electrocardiograms at rest or low-intensity exercise

Vadim Alexeenko[1], Hamid Tavanaeimanesh[2], Freya Stein[2], Jenifer Gold[3], Lauren Hughes[2], Molly McCue[2], Celia Marr [4], Sian Durward-Akhurst[2], Kamalan Jeevaratnam[1]

[1]University of Surrey, UK, [2]University of Minnesota, USA, [3]Wisconsin Equine Clinic, USA, [4]Rossdales Veterinary Surgeons, UK

Cardiac arrhythmias are common in healthy athletic horses and may lead to poor athletic performance or exercise-associated sudden death. Early detection of high-risk horses is an important goal of cardiovascular diagnostics. We hypothesised that non-linear analysis of electrocardiogram disorderliness can be used to identify horses exhibiting intermittent ectopic atrial and ventricular heart rhythm abnormalities at exercise using brief, artifact-free recordings of normal sinus rhythm electrocardiograms collected at sub-maximal heart rates. In a convenience prospective cross-sectional study, ambulatory electrocardiograms were recorded using the Televet 100 or II devices from 110 Thoroughbred or Standardbred racehorses during routine training. Acceptable quality 60-second electrocardiogram strips with stable heart rate (20-120 beats per minute) were identified automatically. Disorderliness of the electrocardiograms was estimated using Lempel-Ziv'76 and '78, and Titchener complexity, and Shannon, sample, and approximate entropy algorithms. Numerical estimates obtained by these algorithms were corrected to the heart rate. For the optimal performance recordings of 60-100 beats per minute should be used, with Lempel-Ziv '76 complexity, R peak and ends of S and T peaks as fiducial points. The receiver operating curve analysis has demonstrated the area under curve of 0.86 for this combination, indicating acceptable differentiation between cases and controls.

C10

New submission

Mahmoud Ahmad Alkahteeb[1], Mohammad Yahya[2], Ghedeir. Alshammari[2], Kawther Amawi[3]

[1]Qatar university, Qatar, [2]KSU, Saudi Arabia, [3]Zarqa Private University , Jordan

Sulfuretin as a Novel Cardioprotective Agent in Type 2 Diabetes: Nrf2-Dependent Protection in a Preclinical Model

Background:
Type 2 diabetes mellitus (T2DM) is frequently complicated by diabetic cardiomyopathy, a major cause of heart failure driven by chronic hyperglycemia, oxidative stress, and inflammation (Kakkar et al., 2025). Despite advances in glycemic control, effective therapies targeting the molecular mechanisms of diabetes-induced cardiac injury remain limited. Sulfuretin, a naturally occurring aurone flavonoid with antioxidant and metabolic regulatory properties, has shown therapeutic potential in metabolic and oxidative stress-related disorders (Li et al., 2025). However, its cardioprotective effects and mechanistic actions in T2DM remain incompletely defined.

Purpose:
This study aimed to evaluate the cardioprotective effects of sulfuretin in experimental diabetic cardiomyopathy in rats with T2DM and to determine the involvement of Keap1/Nrf2 signaling in mediating these effects (Gu et al., 2025).

Methods:
Adult male Wistar rats were assigned to non-diabetic and HFD + streptozotocin-induced diabetic groups (n = 8/group). Each group received vehicle, sulfuretin (5 or 10 mg/kg/day, oral gavage) (Kim et al., 2019), or sulfuretin combined with the Nrf2 inhibitor brusatol (2 mg/kg) (ALTamimi et al., 2023). Cardiac hemodynamics and metabolic indices, as well as cardiac injury markers, lipid peroxidation, antioxidant markers, and several inflammatory mediators, were assessed in the left ventricles of all groups. In addition, cytoplasmic Keap1 and Nrf2, as well as nuclear accumulation of Nrf2, were measured by ELISA, and their expression levels were assessed by qPCR. Finally, hematoxylin and eosin (H&E) staining was performed on left ventricular tissues from all groups to evaluate histopathological changes. Data distribution and homogeneity of variance were evaluated using appropriate normality and variance tests. Intergroup comparisons were performed using one-way or two-way analysis of variance (ANOVA), as appropriate, followed by Tukey's multiple-comparison test. All experiments were conducted in accordance with the approved ethical protocol.

Results:
In diabetic rats, sulfuretin dose-dependently reduced serum levels of CK-MB, LDH, and troponin I and improved cardiac function by reducing LVEDP and increasing LVSP, +dP/dtmax, and -dP/dtmin. Sulfuretin also markedly reduced malondialdehyde (MDA) levels and enhanced total antioxidant capacity, superoxide dismutase, glutathione, and heme oxygenase-1 expression. In addition, it significantly increased the expression and cytoplasmic and nuclear accumulation of Nrf2 in both control and diabetic left ventricles. Furthermore, sulfuretin suppressed tumor necrosis factor-alpha (TNF-alpha) and interleukin-6 (IL-6) levels specifically in diabetic left ventricles and preserved cardiomyocyte architecture. Interestingly, sulfuretin failed to alter glucose, lipid, or insulin levels in non-diabetic animals. All of these functional benefits were abolished by brusatol, confirming Nrf2-dependent cardioprotection.

Conclusion:
Sulfuretin confers robust protection against T2DM-mediated diabetic cardiomyopathy through activation of Nrf2-mediated antioxidant and anti-inflammatory pathways, independent of any hypoglycemic or hypolipidemic effects.

C11

Representations of Heat-Related Bodily Effects among Urban Populations in Accra, Ghana.

Vida Asah-Ayeh[1]

[1]Regional Institute for Population Studies (RIPS) University of Ghana, Ghana

Background

Climate change is a global disturbance that has led to an increase in frequency and intensity of extreme heat events. It poses health risks particularly in vulnerable urban settings (Haines et al, 20006). In sub-Saharan Africa, rapid urbanization, high population density and limited adaptation strategy worsened vulnerability to heat-related health outcomes (Codjoe & Nabie, 2014).

Where extreme heat has been linked to a range of physiological responses, less is known about how affected population represent and understand these effects in everyday contexts. (Kovats & Hajat, 2008).

The study is subsumed within the Heat Adaptation Benefits for Vulnerable Groups in Africa (HABVIA) project, which evaluates heat adaptation and related health outcomes in vulnerable populations (Deglon et al, 2025).

Theoretical perspective

This study draws on Social Representation Theory (Moscovici, 1961) to understand how people make sense of their experiences of extreme heat. It focuses on how these experiences are shared and expressed within the community like Ga-Mashie.

Objective

This study explores community members representation of extreme heat-related bodily effects in Ga-Mashie

Methods

A cross-sectional qualitative design was employed for data collection among 45 participants who were between the ages 18-65 years. They were purposively selected from the Ga-Mashie community, and they were part of the HABVIA project. Data were collected through focus group discussions (FGDs), audio recorded and conducted in Ga language, the primary language spoken in the community. All recordings were transcribed and translated into English for analysis. Ethical approval was obtained. All the participants provided a written informed consent prior to data collection. Thematic analysis was employed to analyze the data.

Findings

Participants accounts provided reflected shared representation of how extreme heat affects the body in multiple ways. They indicated physical exhaustion, characterized by excessive sweating, constantly tired, experience fatigue, headaches, dizziness, blurred vison and skin rashes.

Some of the participants also reported cardiovascular effects, particularly among those with pre-existing hypertension, described experiencing increases in blood pressure and bodily discomfort. Additionally, women highlighted reproductive and hormonal effects, including disruptions in menstrual patterns and worsening menopausal systems during extreme heat periods.

Participants also described perceived causes of extreme heat including environmental change such as cutting down of trees, poor ventilation, overcrowded housing and use of heat producing activities.

Lastly the participants described everyday strategies used to cope with heat like drinking more water, bathing multiple times, using fans and sleeping outdoors at night.

conclusion

The findings show that experiences of extreme heat are understood in different ways, which together forms shared understandings within the community. These shared meanings reflect how people make sense of bodily effects of heat in their everyday lives. Incorporating such community-based accounts into heat-health competence research can develop context-specific responses to heat related health interventions.

C12

Lead is toxic to neuronal cells through induction of oxidative stress and neuroinflammatory pathways.

Khulud Badawi[1], Wayne Carter[1]

[1]University of Nottingham, United Kingdom

Exposure to lead (Pb) is a serious public health concern for which there is no safe level. The aim of this study was to investigate the toxicity of lead to undifferentiated and differentiated human neuroblastoma (dSH-SY5Y) cells and to evaluate gene transcription in response to sub-lethal lead exposure. Pb was applied to undifferentiated and dSH-SY5Y cells across a concentration range of 0-5 mM for 4, 6, and 24 hours, and cell viability was assessed using 3-(4, 5-dimethylthiazol-2-yl)-2, 5-diphenyltetrazolium bromide (MTT) and lactate dehydrogenase assays. Pb induced a significant concentration- and exposure-dependent reduction in cell viability ($p < 0.0001$), with IC50 effects at approximately 3 and 2.5 mM for undifferentiated and dSH-SY5Y cells, respectively. Pb also significantly reduced cellular bioenergetics capacity in a concentration and exposure duration manner ($p < 0.0001$) and resulted in elevated levels of deleterious reactive oxygen species ($p < 0.0001$). RNA sequencing was undertaken to analyse gene transcription in dSHSY-5Y cells in response to a 24-hour exposure to 1.25 mM Pb. Differentially expressed gene (DEG) analysis revealed significant transcriptomic alterations in dSH-SY5Y cells following Pb exposure. A total of 2963 DEGs were identified, of which 757 genes were significantly upregulated, 2206 genes were significantly downregulated, while 26,461 genes showed no significant change. From Gene Ontology analyses, biological processes were predominantly associated with immune and inflammatory responses. From Kyoto Encyclopaedia of Genes and Genomes (KEGG) pathway enrichment analysis, upregulated DEGs were particularly enriched in immune pathways, whereas downregulated DEGs were enriched in pathways related to cellular metabolism, homeostasis, and neurodevelopment. These findings offer molecular insights into Pb-induced neurotoxicity and highlight the potential for Pb exposure to affect both the immune system and neurodevelopment.

C13

HIIT Promotes Autonomic–Metabolic Adaptations

Cristina Blasco-Lafarga[1], Jordi Monferrer-Marín[1], Juan Estevan-Oliver[1], Jørn Wulff Helge[2]

[1]Sport Performance and Physical Fitness Research Group (UIRFIDE), Physical Education and Sports Department, University of Valencia, Valencia, Spain, [2]Department of Biomedical Sciences, Faculty of Health and Medical Sciences, University of Copenhagen, Copenhagen, , Denmark

INTRODUCTION: High-intensity interval training (HIIT) is a safe, time-efficient approach to improve aerobic fitness and performance (Mølmen *et al.*, 2024), even in older adults with reduced metabolic flexibility (Chrøis *et al.*, 2020). Notwithstanding, HIIT adaptations vary across exercise intensities, and their effects on metabolic and autonomic responses remain insufficiently characterized.

This study sought to examine the effects of a 6-week supervised HIIT intervention on metabolic flexibility and cardiac autonomic regulation in active postmenopausal women. Specifically, it aims to examine HIIT training-induced changes in substrate utilization and vagal-related Heart rate Variability (HRV) indices at intensities corresponding to Maximal Fat Oxidation (MFO), and Maximal Carbohydrate Oxidation (MCO) (Monferrer-Marín et al., 2026). The five sit-to-stand-test (5STS) was used as an indicator of lower-limb muscle power and functional performance relevant to activities of daily living.

METHODS: Twenty active women (66.6±6.2 years; 67.9±11.1 kg) volunteered to participate and completed 8 weeks of training of which the last 6-weeks corresponded to a HIIT protocol. (five 1-min bouts at 170–184% of the power output achieved at MCO intensity, interspersed with 1-min active recovery at 0.5 W/kg; 20-min sessions, three times per week). Intensity progressed gradually from 90% to 170% in the two previous weeks.

Experiments were carried out after ethical approval in line with Declaration of Helsinki (2024-FIS-3251696). Statistical analyses and figures were generated using Python 3.13.3 (Python Software Foundation, Wilmington, DE, USA). Normality was tested (Shapiro–Wilk). Paired comparisons were then performed using Student's t-test or the Wilcoxon signed-rank test for body composition, BMR, muscular power, and key metabolic variables at MFO and MCO. Bar plots illustrated variables by intensity domain. Deltas were calculated for efficiency, carbohydrate oxidation, blood lactate, and VO_2 at MCO, and for fat oxidation, SampEn at MFO, and relative power at both intensities. Scatter plots assessed pre–post changes and age effects. Effect sizes were computed using Cohen's d.

RESULTS: At MCO intensity, relative power (d=2.43), Net & Gross efficiency (d=1.26, 1.05), maximal oxygen consumption (d=1.08), respiratory rate (d=0.87), blood lactate (d=0.55), MCO rate (d=0.80) and relative power (d=1.11) increased following HIIT. Stress index also increased (d=0.72). At MFO intensity, maximal fat oxidation rate increased from 0.28±0.09 to 0.32±0.09 g/min (d=0.51), simultaneously with a decrease in perceived exertion (d=0.80), and increased respiratory frequency and sample entropy (d=0.48; d=0.65, respectively).

CONCLUSIONS: Our findings confirm significant beneficial physiological adaptations in active postmenopausal women after a 6-week HIIT program. At FATmax intensity, fat oxidation increased without a shift in the workload corresponding to MFO, accompanied by higher sample entropy. This greater cardiac autonomic complexity may support better fat oxidation regulation. At MCO intensity, improvements were observed in mechanical output, oxygen consumption, carbohydrate oxidation, and blood lactate, together with increased sympathetic activation and higher gross and net efficiency, despite age-related constraints.

Additionally, improvements in relative muscle power (5STS) highlight physiological and functional effectiveness of this short HIIT intervention, supporting its safety and time-efficiency in postmenopausal women. Overall, these results suggest intensity-specific adaptations consistent with enhanced autonomic–metabolic integration.

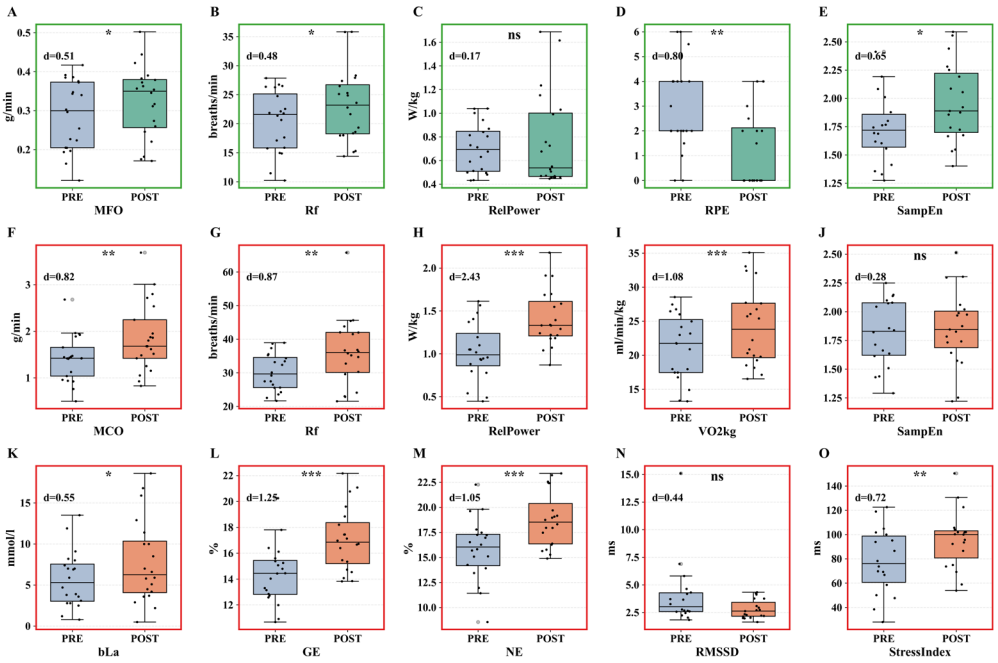

C14

How Do Physiological Networks Determine Survival in Critically Ill Patients with Sepsis?

Akshit Das[1], Alireza Mani[1]

[1]University College London, United Kingdom

Introduction: Redundancy within cardiorespiratory networks is fundamental to maintaining physiological stability under varying conditions. Multiple overlapping control mechanisms ensure that critical functions, such as oxygen delivery, are preserved even when one pathway is compromised. This redundancy enhances system robustness, allowing the body to adapt to stressors such as hypoxia while minimising the risk of failure. This is particularly important in critical illnesses such as sepsis, where impaired physiological network connectivity and sequential organ failure can lead to mortality. Recent advances in network physiology have led to the development of methods for the non-invasive assessment of cardiorespiratory network dynamics. These methods have the potential to evaluate the extent of redundant pathways within the control system and their association with survival in critically ill patients.

Aims: This study aims to use non-invasive methods to assess the extent of redundant pathways involved in cardiorespiratory regulation using the concept of transfer entropy.

Methods: This retrospective study used the Medical Information Mart for Intensive Care III Clinical Database (MIMIC-III), including patients who met Sepsis-3 criteria on admission and had at least 30 minutes of continuous heart rate (HR), respiratory rate (RR), and oxygen saturation (SpO_2) time-series data (n=164). Recording and use of data from the MIMIC-III dataset were approved by the Institutional Review Boards of the participating institutions (IRB Protocol Nos. 2001P001699/14 and 0403000206). This study used the concept of transfer entropy (TE) to quantify information flow among HR, RR, and SpO_2 in critically ill patients with sepsis (1). To assess redundancy, conditional TE was used to determine whether a relationship is truly direct or partly explained by shared dependence on another signal. For example, it was used to evaluate whether TE (HR→RR) reflects a direct link or is influenced by SpO_2, i.e., TE (HR→RR | SpO_2).

Results: Overall, 130 of 164 patients survived at 30-day follow-up. Non-survivors exhibited reduced information transfer (bivariate TE) between physiological variables ($p < 0.05$). Cox regression analysis demonstrated statistical independence for TE (SpO_2→HR), TE (RR→HR), and TE (HR→RR) after adjustment for potential confounders (age, severity-of-disease score, and mechanical ventilation) ($P<0.05$). Increases in these values were associated with reduced mortality (Figure 1). Bivariate TE showed higher mean values than conditional TE, indicating the presence of redundancy within the network (Figure 1). For conditional TE, the prognostic value was less prominent than that of bivariate TE, suggesting that the presence of redundancy in the network may play a protective role in critically ill patients with sepsis.

Conclusion: Physiological network mapping using transfer entropy has the potential to noninvasively measure meaningful interactions among physiological systems, with conditional TE highlighting higher-order interactions and network redundancy that are not captured by bivariate analysis alone.

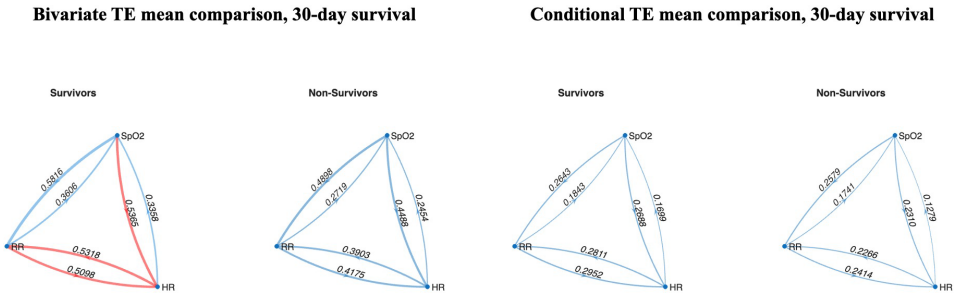

Figure 1. Network maps for survivors and non-survivors, comparing mean values for bivariate TE and conditional TE for each edge. Red: TEs that are predictors of mortality, statistically independent of age, SOFA and mechanical ventilation. Edge weighting corresponds to the magnitude of information transfer. Heart rate (HR), respiratory rate (RR), oxygen saturation (SpO_2), Sequential Organ Failure Assessment (SOFA), transfer entropy (TE).

C15

Tumor blood flow at rest and during exercise in breast cancer patients

Ilkka Heinonen[1], Milla Perros[1], Tiia Koivula[1], Carl-Johan Sundberg[2], Helene Rundqvist[2], Heikki Minn[1], Kari Kalliokoski[1]

[1]Turku PET Centre, Finland, [2]Karolinska Institute, Sweden

INTRODUCTION: It has been suggested and studied that cancer patients would exercise during their chemotherapy drug infusions. The reasoning for that is that pre-clinical studies have shown tumor blood flow (BF) to increase during exercise, which would enhance drug delivery into the tumor. However, this remains sparsely investigated in the clinical setting in cancer patients and was therefore the topic of the present investigation, also because basic physiological responses to physical exercise in the tumor are largely unknown in patients.

AIMS AND OBJECTIVES: The main aim of the present study was to elucidate tumor BF during exercise.

METHODS: Tumor BF was quantified in twenty breast cancer patients with [^{15}O]-H2O positron emission tomography imaging at rest and during supine cycling in the scanner (individually chosen intensity by Borg scale, RPE 11-16). BF was also measured in non-cancerous, contralateral breast tissue. Paired t-test was used for statistical comparisons. The study was approved by the Ethical committee of Hospital District of South-West Finland and patients gave their written informed consent before their participation.

RESULTS: Tumor BF was at rest 12,7±8,5 ml/(dl/min) and during exercise 8,7±8,1 ml/(dl/min), p=0.004. Thus, tumor BF was significantly reduced from rest to during exercise condition. BF in the contralateral healthy breast tissue was much lower and was not significantly changed from rest to exercise (2,0±1,9 ml/(dl/min at rest and 1,6±1,7 ml/(dl/min) during exercise, p=ns).

CONCLUSIONS: To the best of our knowledge this is the first study to investigate tumor blood flow during exercise in breast cancer patients. We report that tumor blood flow is reduced during exercise from the resting baseline in these patients. These results do not support the reasoning that at least breast cancer patients should exercise during their chemotherapy infusions, but whether the responses differ between different cancer patient groups/tumors remains to be investigated. It also remains to be investigated whether tumor blood flow is returned back to baseline after exercise.

C16

Key contribution of the carotid body in preserving cardiac electrical function in chronic hypoxia

Demitris Nathanael[1], Andrew Coney[1], Prem Kumar[1], Andrew Holmes[1]

[1]Department of Biomedical Sciences, School of Infection, Inflammation and Immunology, University of Birmingham, Birmingham, United Kingdom

Introduction. Chronic hypoxia (CH) is a key feature of chronic obstructive pulmonary disease (COPD), an illness associated with increased cardiac arrhythmia risk. CH induces hyperactivity of the carotid bodies which, via increased carotid sinus nerve input to the brainstem, leads to a chronic rise in breathing and heightened sympathetic nerve activity. Whilst it is known that carotid body hyperactivity in COPD patients contributes to vascular dysfunction, a potential role in mediating cardiac electrical remodelling remains uncertain.

Aims and Objectives. The current study assessed ECG parameters in normoxic (N) and chronically hypoxic (CH) animals, before and after acute bilateral carotid sinus nerve section (CSNX).

Method. Recordings of ECG, mean arterial blood pressure (mABP) and respiratory frequency (Rf) were made from adult male Wistar rats (150-350g) following exposure to either 10 days of ambient air (N, n=12 animals) or CH (FiO2=12%, n=13 animals), under alfaxalone anaesthesia (7–12 mg $kg^{-1}h^{-1}$, i.v.), before and after acute CSNX. For N, baseline measurements were made at FiO2=21%, for CH FiO2=12%. A subset of CH animals were treated with relative hyperoxia (FiO2=21%, n=6) after CSNX. Following experiments, animals were killed by overdose of alfaxalone anaesthesia, death confirmed by cervical dislocation. Data presented as mean±SD. Significance taken as $p<0.05$; paired t-test or one-sided Fisher's exact test.

Results. At baseline, CH animals displayed an increase in Rf, a lower mABP, QTc prolongation and shorter QRS duration compared to N. Acute CSNX in N reduced mABP (N: 120±13 vs N+CSNX: 98±17 mmHg, p=0.004, n=12) and Rf (N: 98±12 vs N+CSNX: 82±17 bpm, p=0.0006, n=12), but ECG parameters were unaltered. In CH, CSNX decreased mABP (CH: 95±19 vs CH+CSNX: 78±21 mmHg, p=0.04, n=13) and Rf (CH: 113±12 vs CH+CSNX: 76±13 bpm, p<0.0001, n=13). CSNX also exacerbated QTc lengthening (CH: 68±6 vs CH+CSNX: 76±5 ms, p=0.004, n=13) and increased the occurrence of T-wave inversion (CH: 0/13 vs CH CSNX: 8/13, p=0.0008). 2/8 animals with T-wave inversion exhibited premature ventricular contractions. R-wave amplitude was also depressed by CSNX (CH: 0.36±0.17 vs CH+CSNX: 0.27±0.15 mV, p=0.008, n=13). In a subset of CH animals, treatment with hyperoxia reversed T-wave inversion caused by CSNX (CH+CSNX: 4/6 vs CH+CSNX+hyperoxia: 0/6, p=0.03) and restored the R-wave amplitude (CH+CSNX: 0.23±0.12 vs CH+CSNX+hyperoxia: 0.35±0.11 mV, p=0.01, n=6). However, hyperoxia did not attenuate the exaggerated QTc prolongation (CH+CSNX: 76±6 vs CH+CSNX+hyperoxia: 76±5 ms, p=0.8, n=6).

Conclusions. Complete removal of carotid body sensory input predisposes to pro-arrhythmia ventricular electrical modifications in CH animals. Some of these alterations, including T-wave inversion and R-wave amplitude depression, are likely driven by exaggerated hypoxia following dramatic decreases in Rf. Other modifications such as QTc prolongation which appear O2 insensitive maybe due to changes cardiac autonomic nerve activity. Thus, the carotid body appears to have a heightened protective role in stabilising cardiac electrical activity in CH animals. Potential surgical removal of carotid bodies to improve vascular function in patients with COPD should be viewed with caution.

C17

How Do Physiological Networks Change Prior to the Onset of Acute Mountain Sickness?

Baoer Lin[1], Thomas Williams[2], Charles Taylor[2], Joseph Costello[2], Ali Mani[1]

[1]Network Physiology Laboratory, UCL Division of Medicine, University College London, London, UK, United Kingdom, [2]Extreme Environments Laboratory, School of Psychology, Sport and Health Sciences, University of Portsmouth, Portsmouth, UK, United Kingdom

Background: Acute mountain sickness (AMS) is a common condition at high altitude, presenting with symptoms such as headache, fatigue, and, in severe cases, life-threatening pulmonary or cerebral oedema. Predicting the occurrence of AMS using standard clinical metrics remains challenging. Network physiology is a multidisciplinary field that explores the collective behaviour of physiological systems and may offer a novel approach to understanding AMS by visualising and quantifying the complex interactions and information exchange between these systems.

Aim: This study aims to explore how physiological networks change during 11 hours of normobaric hypoxia and whether causal information flow within the cardiorespiratory system differs between individuals who develop symptoms of AMS and those who do not.

Method: All experimental procedures were approved by the Science and Health Faculty Ethics Committee of The University of Portsmouth (project no. SHFEC 2024-034). A convenience sample of ten individuals provided their written informed consent to participate in this study (9 male and 1 female, age: 26.5±5.9). The participants underwent 11 hours of normobaric hypoxia (FiO_2= ~0.12) while the following physiological signals were recorded: heart rate (HR), respiratory rate (RR), tidal volume (VT), minute ventilation (VE), end-tidal CO_2 ($PetCO_2$), end-tidal O_2 ($PetO_2$), and capillary oxygen saturation (SpO_2). Transfer entropy was used to construct causal network maps, measuring the directed information exchange between time-series variables (1). The Lake Louise Acute Mountain Sickness Questionnaire (LLS) was used to assess the development of AMS. An LLS score of ≥ 3, in the presence of headache and at least one other symptom, indicates AMS (n = 5). Some participants exited early because they were unable to complete the 11 hours of hypoxia.

Results: Two-way ANOVA results (n=10) showed no significant difference between mean values of measured physiological variables between AMS and Non-AMS group throughout hypoxia hours, suggesting that cardiorespiratory signals alone may fail to predict AMS onset. Network analysis revealed some topological differences between groups; Qualitatively, non-AMS group exhibited a more connected network with highly integrated information exchange, suggesting better physiological adaptation. The AMS group showed a progressive decoupling of physiological nodes while this was potentially confounded by participants' attrition as they developed AMS and exited at different hours. Specifically, SpO_2 and HR nodes, main information receiving (indegree) nodes at the baseline hour (FiO_2=21%), experienced a notable decrease as participants entered hypoxia for both groups. To account for different AMS participants' exit time due to AMS onset, Event–Locked Analysis was performed, resetting the baseline to AMS event onset. Results showed qualitatively that the system underwent significant uncoupling in the hours preceding AMS, characterized by SpO_2 and HR's visible indegree reduction, suggesting less information exchange under prolonged hypoxia. The uncoupling may be further supported by the decrease in information sent between all variables in hours before AMS compared to baseline. There was no statistical difference in indegree and outdegree between the groups.

Conclusion: Physiological network mapping has the potential to visualise adaptive responses to physiological stressors, such as prolonged hypoxia, in order to develop physiological markers for the early detection of AMS.

C18

Spatiotemporal inhomogeneity of the sarcomere in the beating hearts captured by the phase-targeting cryofixation technique

Kentaro Mochizuki[1], Shoko Tamura[1], Yasuaki Kumamoto[2], Yuma Morishita[1], Masahito Yamanaka[2], Wen-Jin Ho[1], Yoshinori Harada[1], Katsumasa Fujita[2], Hideo Tanaka[3]

[1]Kyoto Prefectural University of Medicine, Japan, [2]The University of Osaka, Japan, [3]Kyoto University of Advanced Science, Japan

Introduction

The heart exhibits organized excitations and contractions as a physiological syncytium comprised of numerous cardiomyocytes. However, the extent to which myocyte structural arrangement varies across cardiac phases remains unknown.

Aims and objectives

We aimed to visualize the spatiotemporal variance of sarcomere length (SL) in the subepicardial myocardium of the beating heart at a histological scale. To capture snapshots of the SL distribution across the myocardium during systole and diastole, we performed rapid cryofixation with phase-targeting in isolated rat hearts [**Ref.**].

Method

Using a home-built cryogen-ejection system, the Langendorff-perfused rat heart was rapidly frozen during peak systole or end diastole under electrical pacing at 0.5 Hz. Figure 1 shows sequential side-view photographs of the heart in the rapid freezing during peak systole. The frozen heart, subsequently fixed with paraformaldehyde (PFA) and acetone by a freeze-substitution procedure, was immuno-stained to visualize α-actinin of sarcomere structures (i.e., Z-line). Fluorescence image of the Z-line in myocytes of the subepicardial myocardium (>44,000 μm^2/image) was obtained via confocal laser-scanning microscopy. The representative value of SL for each myocyte was calculated from the Fourier transform of the line profiles of the Z-line cycle. To visualize the local SL distribution in myocytes, heatmaps were reproduced from the fluorescence images of Z-lines. All animal experiments were approved by the Animal Research Committee of Kyoto Prefectural University of Medicine. Hearts were excised (i.e., euthanasia) from Wistar rats (male, 9-13 weeks old) under deep general anesthesia.

Results

In the fluorescence images of hearts prepared via phase-targeting rapid cryofixation, the Z-lines in myocytes appeared closely spaced in the hearts rapidly frozen during peak systole (RF-systole) as opposed to those frozen during end diastole (RF-diastole). Statistically, the SL of RF-systole (1.57 ± 0.12 μm, n = 5 hearts) was significantly shorter than that of RF-diastole (1.92 ± 0.14 μm, n = 5), as determined via one-way ANOVA followed by Tukey post-hoc test for multiple comparisons ($P < 0.05$). The SL of RF-

diastole was comparable to that of the rapidly frozen hearts under pharmacological relaxation with 2,3-butanedione monoxime (RF-BDM-diastole: 1.97 ± 0.11 µm, n = 3) and hearts fixed by PFA-perfusion (1.82 ± 0.11 µm, n = 3). However, detailed examination of the localized SL distribution using heatmaps unveiled that the individual SL of RF-systole was nearly uniform and shorter, but showed some local longer regions (Figure 2, Scale bar: 50 µm). In contrast, the RF-diastole revealed the predominant SL elongation with patchy distributions of shorter regions. These local regions are highlighted with dotted-circles in both middle panels to ensure accessibility. Such SL spatial inhomogeneity was not seen in RF-BDM-diastole and PFA-fixed hearts. Additionally, we succeeded in obtaining snapshots of spatiotemporally chaotic SL dynamics in the heart during ventricular fibrillation via rapid-freezing, which was not possible with the conventional PFA fixation.

Conclusions

Phase-targeting rapid cryofixation of the beating heart enabled spatiotemporal and histological analysis of myocyte structures, which is difficult to achieve through conventional live imaging due to a trade-off between temporal resolution and the available signal. Our strategy will help investigate spatiotemporal changes of cardiac structures and associated physiological functions.

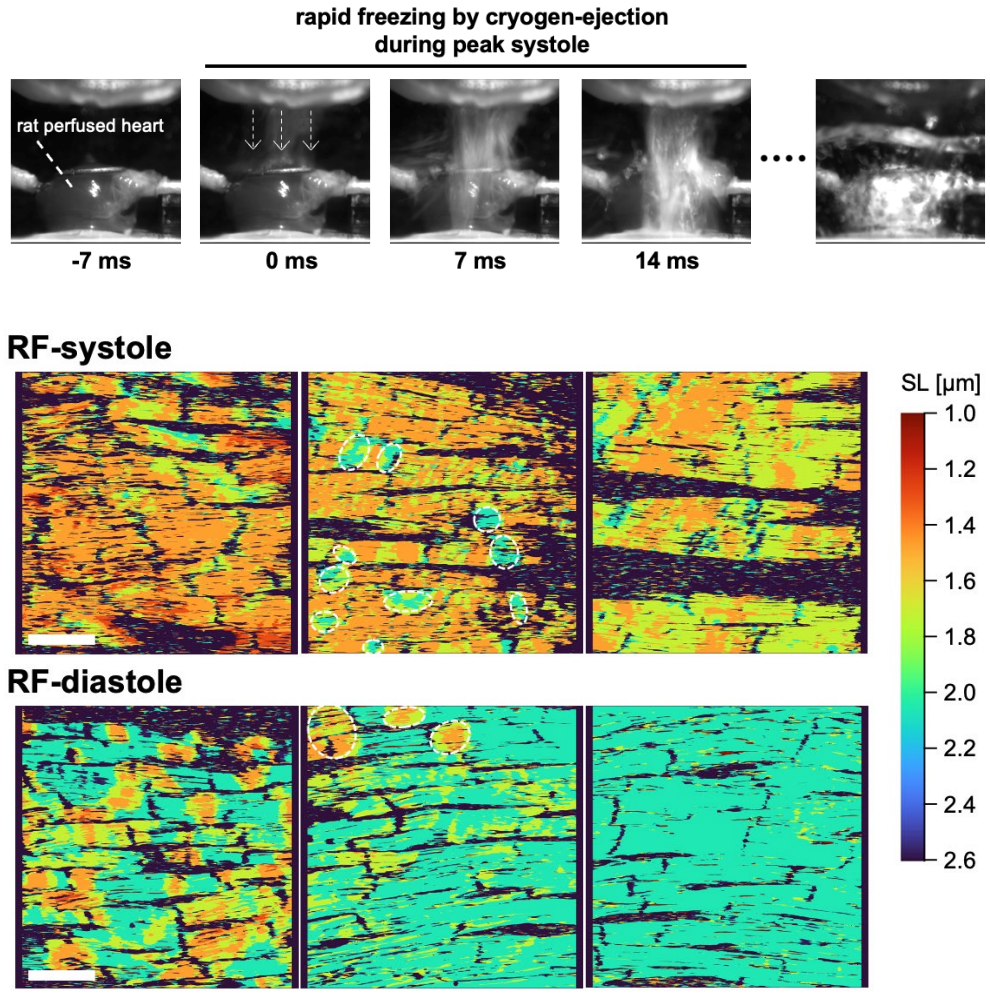

C19

Autonomic Function and Metabolic Flexibility: A Dynamic Cross-Correlation Analysis

Jordi Monferrer-Marín[1], Juan Estevan-Oliver[1], Jørn Wulff Helge[2]

[1]Sport Performance and Physical Fitness Research Group (UIRFIDE), Physical Education and Sports Department, University of Valencia, Valencia, Spain., Spain, [2]Department of Biomedical Sciences, Faculty of Health and Medical Sciences, University of Copenhagen, Copenhagen, Denmark, Denmark

INTRODUCTION: Aligned with the idea of a vagal cardiometabolic-autonomic link, nonlinear heart rate variability has been proposed as an early marker of metabolic alterations (Zamora-Justo *et al.*, 2025), and resting vagal activity has been associated with maximal fat oxidation (MFO) in postmenopausal women (Monferrer-Marín *et al.*, 2024), This population is often characterized by age- and oestrogen-related metabolic and autonomic impairments, including reduced fat oxidation (Abildgaard *et al.*, 2013) and lower vagal HRV indices (Giunta *et al.*, 2024). However, the dynamic interaction between autonomic regulation and substrate utilization during exercise remains poorly characterized in this population.

AIM: This study aimed to examine the interaction between vagal and sympathetic activity and energy substrate utilization during an incremental exercise test in active postmenopausal women.

METHODS: Seventy-eight active postmenopausal women (68.2±5.4 years; 66.3±11.2 kg) completed a two-day cross-sectional protocol involving a graded FATmax test with indirect calorimetry and heart rate variability (HRV) monitoring. Primary outcomes focused on FATox and its autonomic correlates, defined as heart rate variability indices reflecting short-term fractal correlation properties (DFAα1) and vagal modulation (RMSSD), while secondary analyses assessed the coupling between CHOox and linear autonomic indices, including a geometric HRV-derived metric reflecting sympathetic predominance as Stress Index and also RMSSD. Time-series were normalised to the percentage of test duration. Dynamic cross-correlation matrices, and exponentially weighted moving-average rolling correlations (|r|), a time-resolved method to assess dynamic associations between variables.

RESULTS: RMSSD displayed the strongest temporal association with FATox (|r| = 0.62), DFAa1 showed moderate dynamic correlation (|r| = 0.40), and SampEn exhibited weak and unstable correlations. In contrast, CHOox demonstrated stronger and more stable associations with autonomic indices, being inversely associated with RMSSD (|r| = 0.87) and positively linked to the Stress Index (|r| = 0.84).

CONCLUSIONS: Data reveal an intensity-dependent association between autonomic dynamics and substrate utilization during exercise in active postmenopausal women. Fat oxidation shows a consistent relationship with vagal indexes, whereas carbohydrate oxidation is associated with vagal withdrawal and sympathetic activation markers. CHOox associations appear stronger, likely reflecting its faster kinetics compared with FATox and closer temporal alignment with autonomic fluctuations. Overall, these findings support the presence of coordinated, yet intensity-dependent, autonomic–metabolic interactions shaping exercise responses in this population.

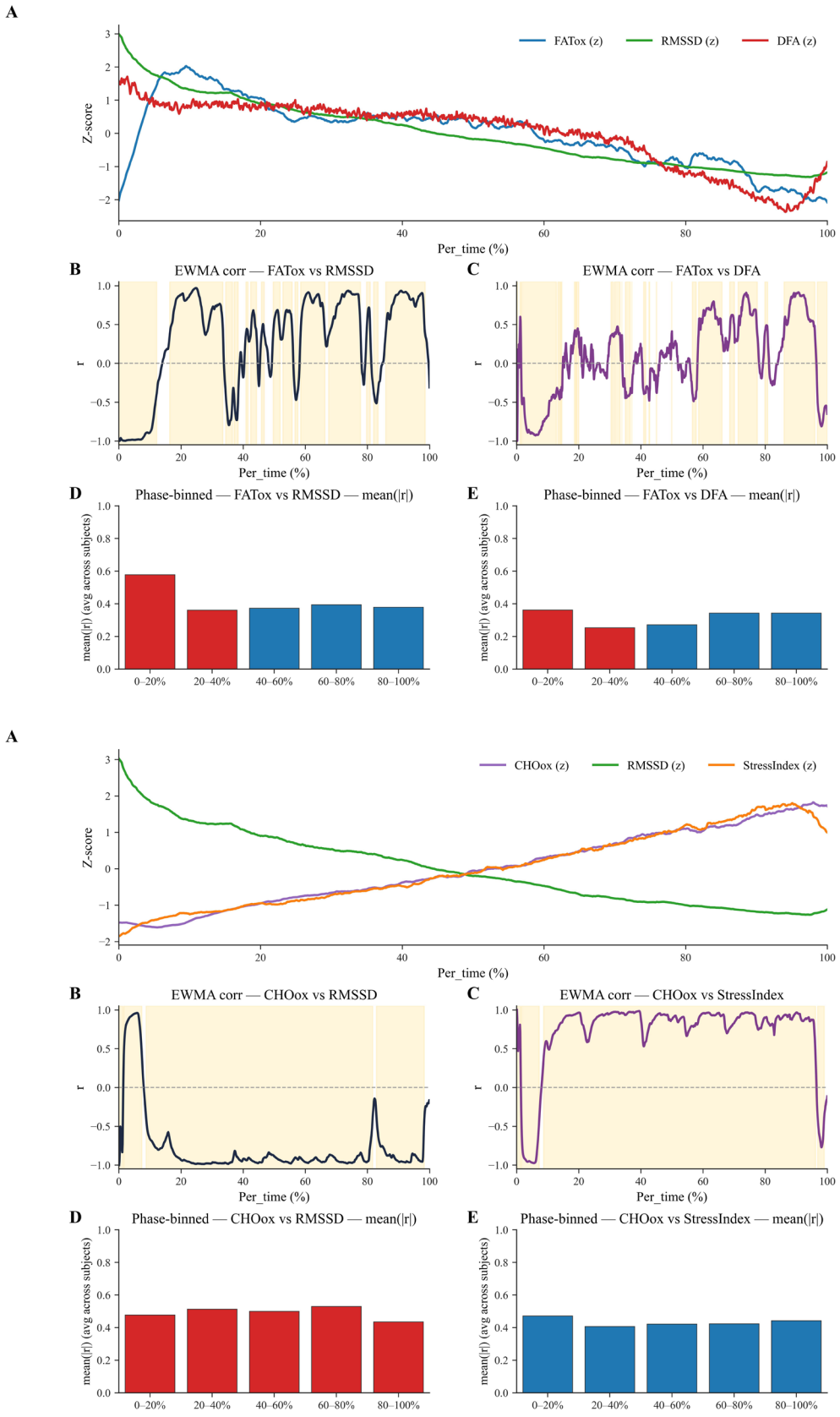
A
FATox (z)
RMSSD (z)
DFA (z)
Z-score
Per_time (%)
B
EWMA corr — FATox vs RMSSD
r
Per_time (%)
C
EWMA corr — FATox vs DFA
r
Per_time (%)
D
Phase-binned — FATox vs RMSSD — mean(|r|)
mean(|r|) (avg across subjects)
0–20%
20–40%
40–60%
60–80%
80–100%
E
Phase-binned — FATox vs DFA — mean(|r|)
mean(|r|) (avg across subjects)
0–20%
20–40%
40–60%
60–80%
80–100%

A
CHOox (z)
RMSSD (z)
StressIndex (z)
Z-score
Per_time (%)
B
EWMA corr — CHOox vs RMSSD
r
Per_time (%)
C
EWMA corr — CHOox vs StressIndex
r
Per_time (%)
D
Phase-binned — CHOox vs RMSSD — mean(|r|)
mean(|r|) (avg across subjects)
0–20%
20–40%
40–60%
60–80%
80–100%
E
Phase-binned — CHOox vs StressIndex — mean(|r|)
mean(|r|) (avg across subjects)
0–20%
20–40%
40–60%
60–80%
80–100%

C20

Ventilatory consequences of fentanyl and xylazine co administration on CD1 mice assessed by whole body plethysmography

Rebecca Okubadejo[1], Eamonn Kelly[1], Ana Paula Abdala Sheikh[2], Graeme Henderson[1], Emma Hart [2]

[1]School of Physiology, Pharmacology and Neuroscience, University of Bristol, United Kingdom, [2]Bristol Medical School, University of Bristol, United Kingdom

Introduction

Xylazine, an α_2-adrenoceptor agonist and veterinary sedative, has increasingly appeared as an adulterant in illicit fentanyl supplies, raising significant public health concerns regarding its effects on ventilatory control. While fentanyl is well known to cause profound ventilatory depression in humans; xylazine's effect is less well studied.

Aims and Objectives

In this study, we aimed to determine how xylazine and fentanyl, individually and in combination, affect respiratory regulation in adult mice. We also evaluated the ability of the antagonists atipamezole (for xylazine) and naloxone (for fentanyl) to reverse these effects. We hypothesised that non-toxic doses of xylazine would exacerbate fentanyl-induced ventilatory depression, and that a combined atipamezole-naloxone intervention would be required to reverse respiratory impairment following co-drug exposure, reflecting emerging clinical reports of xylazine attenuating naloxone's effectiveness[1].

Methods

Unrestrained whole-body plethysmography[2] was used to record ventilatory parameters including breathing frequency, tidal volume, minute ventilation, inspiratory and expiratory times (Ti and Te), and peak inspiratory and expiratory flows (PIF and PEF). Adult male and female CD1 mice received intraperitoneal injections of either xylazine (3 or 10 mg/kg) or fentanyl (0.05, 0.15, or 1.35 mg/kg), and their respective antagonists (1 mg/kg naloxone; 3 mg/kg atipamezole), the latter given 20 minutes post-drug. N was 6 per experimental group. Co-administration experiments used 0.15 mg/kg fentanyl with 3 mg/kg xylazine. All experiments were carried out in accordance with the UK Animals (Scientific Procedures) Act 1986 and were approved by the University of Bristol's Animal Welfare Review Body. Data were normalised to baseline (first 10 minutes), area under the curve calculated and these processed to generate mean parameter-per-minute values. Statistical significance was assessed using one-way ANOVA with Šídák's post-hoc test.

Results

Either fentanyl or xylazine alone produced pronounced ventilatory depression through distinct alterations of the ventilatory cycle. High-dose fentanyl (1.35 mg/kg) markedly prolonged Ti (167% of baseline), whereas xylazine (10 mg/kg) significantly increased Te (197%), with both changes reducing ventilation rate ($p < 0.05$). Minute ventilation decreased in a dose-dependent manner for both drugs, with xylazine producing slightly greater suppression at the highest dose (60% vs. 50%). Fentanyl increased the Ti/Te ratio (+65%), while xylazine reduced it (-30.5%). Co-administration produced similar effect sizes on Ti and Te to the individual drugs but caused a significantly greater reduction in the PIF/PEF ratio (-34%, $p < 0.01$), exceeding that induced by fentanyl alone (-24%), indicating a stronger combined impairment of inspiratory function. Only the combined naloxone-atipamezole treatment fully restored ventilation rate to baseline after co-administration ($p < 0.01$). All antagonist treatments improved Ti/Te and PIF/PEF ratios,

with the strongest improvements observed following naloxone alone and the combined therapy ($p < 0.001$).

Conclusion

These findings underscore the clinical complexity of xylazine-fentanyl co-use and the heightened risk of overdose, emphasising the need for updated treatment strategies. Ongoing work using the working heart-brain preparation[3] aims to identify the central mechanisms underlying the drugs' divergent ventilatory effects.

C21

The normalization of tissue and organ function by Ou MC decrescendo phenomenon and spatial awareness

Ming Cheh Ou[1], Chung Chu Pang[2], Yi Jen Ou[3]

[1]Taipei City Hospital, Taiwan, [2]National Taiwan University, Taiwan, [3]Fuhsing Private School, Taiwan

Background: Ou MC decrescendo phenomenon shows to be an intracorporeal interoceptive issues yielded by interactions of human body anatomical axes (HBAAs). Spatial awareness may contbutes the effect of interoceptive sensation by Ou MC decrescendo phenomenon [1].

Methods & Results: Ou MC decrescendo phenomenon exercise with left to right and dorsoventral axis interactions yields interoceptive issues which alleviates pain, causes cessation of uterine bleeding, improves organ dysfunction, depresses malignancy of cancer. Three-dimension is more effective than two-dimension HBBAs interactions [1]. Nonetheless, the interoceptive sensation by the spatial awareness meditation (walking or mirror) of the spatial schema of human body also showed to improve muscular phasic activity, postural coordination and stiffness for locomotive deterioration of aged patients [2,3].

Discussions: The effect of Ou MC decrescendo phenomenon is related to the interactions of HBBAs which yield anti-inflammatory reaction in our studies [1]. While the patients perform Ou MC decrescendo phenomenon exercise, the interactions of HBBAs apparently cause an intracorporeal spatial awareness and yield interoceptive sensation. Nonetheless, the spatial awareness by meditation for the schema of human body also yields interoceptive sensations with similar effect [2,3]. Probably, a spatial awareness by meditation is related to HBBAs of the schema of human body. Further studies are warranted.

C22

Lifetime stress and blood pressure in Black and White females

Madelaine West[1], Hazel C. Blythe[2], Ian D. Driver[3], Abimbola Aiku, Kevin Murphy[4], Angus K Nightingale[5], Emma C. Hart[2], Lydia L. Simpson[2]

[1]University of the West of England, United Kingdom, [2]University of Bristol, United Kingdom, [3]Cardiff University, United Kingdom, [4]Cardiff University , United Kingdom, [5]University Hospitals Bristol and Weston NHS Foundation Trust,, United Kingdom

Background: Females of Black African and Black Caribbean heritage have higher rates of hypertension and experience greater end-organ damage compared with other ethnic groups. Blood pressure (BP) reactivity, 24-hour ambulatory BP variability and nighttime BP dipping are prognostic for future cardiovascular disease and stroke and are altered in Black females. Greater lifetime stress exposure may contribute to these health disparities; however, its effects on BP reactivity, ambulatory BP variability and nighttime BP dipping remain unclear.

Methods: We examined associations between lifetime stress and BP parameters in Black and White female volunteers. Seventeen healthy Black females (37±12yrs, BMI: 24.8 ± 4.0kg/m^2) and 17 age and BMI-matched White females (37±13yrs, BMI: 24.6 ± 4.3kg/m^2) completed a mental arithmetic task, 24-h ambulatory BP monitoring and venous blood sampling. Resting BP, Peak BP response to a mental arithmetic task, average real variability (ARV) in 24-hour BP (calculated as mean of absolute differences between successive readings) and BP dipping (absolute dip and nighttime:daytime BP ratio) were measured. The Stress and Adversity Inventory (STRAIN) was used to assess total lifetime stress count (StressC) and total lifetime stress severity (StressS), as well as early-life adversity stress count (Early StressC) and early-life adversity stress severity (Early StressS), alongside resting cortisol levels. Data were compared using T-tests or Mann Whitney U, and associations between BP parameters and STRAIN scores were assessed using Pearson correlation. Data are presented as mean ± SD

Results: There was no difference in resting systolic (115±9 vs 116±6 mmHg, P=0.880) and diastolic BP (76±7 vs 76±6 mmHg, P=0.757), peak BP reactivity (SBP Δ19±13 mmHg vs Δ23±16 mmHg, P =0.335; DBP Δ12±9 vs Δ13±4 mmHg, P=0.712) and 24-hour ARV in SBP (9.9±2.2 vs 10.8±2.5 mmHg, P=0.323) and DBP (7.4±1.9 vs 8.3±1.8 mmHg, P=0.236) between Black females and White females. However, Black females exhibited an attenuated nighttime systolic (Δ-9±7 vs. Δ-12±7mmHg, P=0.034) and diastolic (Δ-11±4 vs. Δ-14±4mmHg, P=0.024) BP dipping and a greater systolic (0.93±0.06 vs 0.88±0.06 P=0.024) and diastolic (0.86±0.04 vs 0.81±0.05 P=0.022) dip ratio. Resting cortisol levels (175.3±133.7 vs 195.8±97.3nmol/L, P=0.152) lifetime stress exposure (StressC: 23±16 vs 18±10, P=0.166; StressS: 58±32 vs 40±19, P=0.099) and early-life adversity stress scores (Early StressC: 5±6 vs 4±3 , P=0.415; Early StressS: 14±12 vs 9±6, P=0.159) were not different between groups. STRAIN scores were not correlated with nighttime BP dipping or BP reactivity in either group (P>0.05). However, lifetime stressor count (Black females r=-0.57, P=0.026; White females r= -0.69, P=0.003) and lifetime stressor severity (Black females r=-0.56, P=0.023; White females r =-0.64, p=0.007) were negatively correlated to 24-hour DBP ARV in both groups, with early adversity stress count (Black females r=-0.64, P=0.009) and severity (Black females r=-0.74, P=0.002) also correlated with 24-hour DBP ARV in Black females, but not White females.

Conclusion: Our findings suggest that lifetime stress exposure may contribute to BP variability in females, with early-life adversity also associated with BP variability in Black females. Further research is required to determine how stress exposure BP variability influence cardiovascular and stroke risk, particularly in Black females.